

# Quantitative extraction and analysis of carriers of magnetization in sediments

Mark W. Hounslow and Barbara A. Maher

*School of Environmental Sciences, University of East Anglia, Norwich NR4 7TJ, UK*

Accepted 1995 July 3. Received 1995 May 25; in original form 1995 January 11.

## SUMMARY

We have applied an integrated procedure for quantitative magnetic mineral extraction, based on the separation method of Petersen, von Dobeneck & Vali (1986), to a range of sediment types, to examine the efficiency and representative nature of the extraction process. Carriers of magnetization have been identified by rock magnetic measurements, microscopy and X-ray diffraction. Quantification of the extraction efficiencies is achieved by before- and after-extraction rock magnetic measurements (susceptibility, anhysteretic and isothermal remanences). These magnetic measurements show that our modified extraction method extracts large proportions of the magnetization carriers in a range of sediment types (e.g. over 75 per cent for magnetite-dominated sediments). The extraction efficiency is dependent on the sample magnetic mineralogy and whether the magnetic grains occur as discrete grains or as inclusions within host grains. Susceptibility extraction efficiencies are strongly dependent on whether the susceptibility is of paramagnetic or ferrimagnetic origin. The amount of material recovered in the extract shows some inverse correlation with the density of the sediment suspension used during extraction.

In terms of the mineralogies extracted, we identify a diverse and complex range of mineral assemblages. All sizes of discrete grains of magnetite are extracted (including single-domain and superparamagnetic grains, and chains of bacterial magnetite). Other commonly extracted iron and titanium oxides are haematite and ilmenite. Ferrimagnetic chromites and sulphides were also obtained from some samples. Considerable amounts of quartz and feldspar are extracted, due to the presence of magnetic inclusions within these diamagnetic host grains. In the deep-sea sediments we examined, feldspars constitute a large proportion of the extracts, but are significantly less abundant in other sediments, where quartz is dominant. A wide variety of paramagnetic minerals was identified in the extracts, including pyroxenes, amphiboles, chlorites, micas, Mg–Cr-spinels, garnets, Ti-oxides, apatites, tourmaline and zircon, many of which contain ferrimagnetic inclusions, possibly less than 0.1  $\mu\text{m}$  in grain size.

Dissolution of ultrafine grains of magnetite during pre-extraction carbonate dissolution, as suggested by Sun & Jackson (1994), does not occur in our samples.

**Key words:** haematite, magnetic susceptibility, magnetite, marine sediments, palaeomagnetism, paramagnetism, remanent magnetization.

## INTRODUCTION

Palaeomagnetic and rock magnetic studies of sediments and soils rely on the presence of small amounts of ferrimagnetic and canted-antiferromagnetic minerals which carry measurable remanent and induced magnetic properties. The sensitivity of current instrumentation is such that the remanent magnetization due to less than one ppb ( $10^{-9}$ ) of magnetite can be measured. The advantage of rock magnetic analyses of rocks,

sediments and soils is that samples can be characterized quite rapidly and distinctively, with the possibility of high-resolution discrimination of environmental change, as recorded by variations in the measured magnetic properties. For instance, magnetic signatures of deep-sea sediments and of continental loess deposits record precisely the imprint of global climate change during the Cenozoic (Bloemendal & deMenocal 1989; Robinson 1990; Maher & Thompson 1992; Maher, Thompson & Zhou 1994).

Interpretation of variations in rock magnetic (and palaeomagnetic) properties in terms of environmental processes depends heavily upon inferences about the origins of the magnetic minerals. The origins of the magnetic minerals may be identified by examination of their morphology and chemical compositions, and their relationship with other mineral components. Such physical and chemical characterization of natural magnetic particles preserved in sediments and soils has so far not kept pace with the proliferation of rock magnetic measurements. Rock magnetic data cannot normally identify uniquely the precise mineralogy and source of the carriers of magnetization. This is exemplified by the current debate about the origin of magnetic minerals and the rock magnetic signature, in remagnetized Palaeozoic carbonates (Lu, Marshek & Kent 1990; Jackson *et al.* 1993; Suk, Van der Voo & Peacor 1993; McCabe & Channell 1994; Sun & Jackson 1994).

To identify the sources of the remanent magnetization properties of sediments and soils, two approaches can be taken. One is to examine the magnetic grains *in situ*. Where samples contain magnetic grains larger than  $\approx 1 \mu\text{m}$ , this can be done by optical and/or scanning electron microscopy (SEM) of polished sections (e.g. Walker, Larson & Hoblitt 1981). When the magnetic grains are submicron in size, thinned sections can be prepared using ion-beam milling, for subsequent analysis by transmission electron microscopy, TEM (Morgan & Smith 1981; Geissman, Harlan & Brearley 1988). This approach gives information on mineralogy and also mineral interrelationships. However, it can only readily be applied to samples containing a high concentration of magnetic grains and/or grains larger than  $\approx 1 \mu\text{m}$ , as small numbers of sub-micron particles are difficult to detect.

The second approach is to remove the magnetic grains from the sample (thereby possibly losing the information on mineral interrelationships) by some magnetic extraction procedure, and to analyse the magnetic grains by microscopy, X-ray diffraction and elemental analysis.

These analyses are more time-consuming than rock magnetic measurements, but enable a more detailed understanding of the sources of the magnetic minerals and the causal links between environmental change, rock magnetic variations and the palaeomagnetic signal. They also allow structural, physical and chemical characterization of natural magnetic minerals, which will lead to enhanced understanding and interpretation of rock magnetic data.

We present here results from a variety of sediment samples subjected to quantitative magnetic mineral extraction. Improved extraction efficiency, quantification of the extraction procedure, and subsequent analysis of the minerals extracted, combine to enable more detailed and representative assessment of the magnetic mineralogy. In addition, quantification allows assessment of the limitations and any selective bias of the extraction procedure.

## MAGNETIC EXTRACTION TECHNIQUES

Magnetic extraction techniques rely on the generation of a magnetic field gradient, within which the magnetic grains are trapped (Schulze & Dixon 1979; Von Dobeneck 1985). Within any sample, there is likely to be a wide variety of minerals: diamagnetic, paramagnetic, antiferromagnetic and ferrimagnetic minerals. In palaeomagnetic or rock magnetic studies, it is generally the ferrimagnetic minerals which are of most

significance, so any extraction procedure should concentrate these into a separate, with as little contamination as possible by other non-remanence carrying magnetic minerals. However, in studies of clays (e.g. Righi & Jadualt 1988) or other minerals, magnetic extraction procedures can be designed to concentrate the paramagnetic or antiferromagnetic minerals (Schulze & Dixon 1979).

In palaeomagnetic and rock magnetic studies, three types of magnetic extraction procedure have been used (Table 1). Each of these methods is best suited for removing particular types of magnetization carriers or grain sizes. We describe here the use of all three separation procedures, in an integrated approach to the analysis of magnetic minerals. This approach can be used not only for examining the remanence-carrying phases, but also the paramagnetic minerals, which can be important contributors to the susceptibility in some sediments and soils.

### Are magnetic extracts representative of the original sample?

In considering how representative a magnetic extract is of its parent sample, the purpose of investigation must be borne in mind. For environmental magnetic studies, an unbiased subset of all the grain sizes and magnetic minerals should be representative. However, for studies of natural remanences, where a sub-population of magnetic grains may carry the important palaeomagnetic signal, both artificial remanences and magnetic extractions may not uniquely discriminate those grains.

It is often implicitly assumed in magnetic extraction studies that the magnetic separation removes a representative suite of magnetic grains from the sample. However, this ideal magnetic separation is unlikely to be achieved easily, since the extraction procedure is dependent upon many factors such as field gradient, flow rate, magnetic grain size and textural relationships (e.g. discrete grains versus intergrowths), sample composition and suspension concentration (Cummins *et al.* 1976; Schulze & Dixon 1979; Von Dobeneck 1985). It is normal for the magnetic separation to introduce selective bias into the amount of magnetic material extracted, its grain size and the relative amounts of paramagnetic and ferrimagnetic grains removed. Differences in magnetic field magnitude, gradient and sample flow rate primarily control the types of magnetic particles removed by extraction (Cummins *et al.* 1976). For example, the three types of magnetic separation shown in Table 1 would likely produce quite different quantities and grain sizes of minerals from the same sample, because of the interplay of these physical parameters.

Separation bias was demonstrated by Sun & Jackson (1994) who showed that the procedure they used did not remove the magnetic grains which gave rise to the characteristic 'waspy' hysteresis loops of their samples. Similarly, on the basis of their rock magnetic data, Bloemendal *et al.* (1993) suspected the presence of ultrafine biogenic magnetite within the surficial sediments of ODP Hole 722B (Owen Ridge, Indian Ocean). However, they were unable to observe any such grains in their magnetic extracts.

Therefore, when using any magnetic separation procedure, it is most important to determine how much bias the magnetic extraction introduces into the final collection of grains called 'the extract'. We have done this by using rock magnetic measurements before and after the extraction procedure to

Table 1. Magnetic extraction procedures used in magnetic and clay mineral studies.

Magnetic extraction procedure	Characteristics	Mineralogy/Grain sizes preferentially extracted	References
Magnetised probe (MP)	Relatively low magnetic field (<~100mT), high magnetic field gradient at end of magnetised probe (Fig. 2). Sample circulated in suspension over probe for several days.	All sizes of ferrimagnets	Petersen et al., 1986 von Dobeneck et al., 1987 Vali et al., 1989
Magnetic edge (ME)	Magnetic field gradient generated at edge of pole pieces of electromagnet, or permanent magnet. Commonly, suspensions passed through tubes attached to electromagnets.	Ferrimagnets (>~1µm) + paramagnets + antiferromagnets	Lovlie et al., 1971 McCabe et al., 1983 Freeman, 1986 Canfield and Berner, 1987 Karlin, 1990
'High-gradient' (HG)	Stainless steel wire packed into tubes, placed in a large (~1T) magnetic field, field gradients generated at wire edges. Sample suspension passed through the tubes.	Paramagnets+ ferrimagnets (>~1µm) + antiferromagnets	Hughes, 1982 Righi and Jadault, 1988 Sun and Jackson, 1994

quantify any bias, and also to determine how much magnetic material has been removed from the host sediment at each extraction stage. The mineralogy of the resulting extracts has been assessed by use of X-ray diffraction, optical and electron microscopy.

## SAMPLES AND EXPERIMENTAL TECHNIQUES

The results presented here are for a range of geological samples from several locations (Table 2). Most of the samples, with the exceptions of the Lunde sandstones and the UK Pleistocene samples, have mean clastic grain sizes finer than coarse silt. Except for the UK Pleistocene specimens, the samples con-

tained carbonate, either as detrital components (ODP samples and Cretaceous chalk) or as diagenetic cements (Lunde formation). This was removed by a buffered acetic acid pre-treatment (2M, pH 4.5; Freeman 1986; Fig. 1). Initial extraction experiments indicated the presence of significant amounts of ferrimagnetic contaminants in even the high-quality reagents used; consequently all reagents used in the extraction procedure were pre-filtered (0.2 µm filter) to ensure non-contaminated extracts.

## Magnetic separation

We use a sequential magnetic separation procedure that potentially gives four magnetic separates from each sample,

Table 2. Details of the samples used for the magnetic extraction.

Sample	Sample Depths	Location	Lithology	Age	References
ODP Leg 117, Hole 722B	0.35-60m	Owen Ridge, Indian Ocean, water depth 2028m	Foraminiferal ooze, carbonate content 50-80%	Pleistocene to upper Pliocene	Prell et al., 1989
ODP Leg 117, Hole 724C	0.3-50m	Oman margin, Indian Ocean, water depth 593m	Clayey, calcareous silt, carbonate content 30-80%	Pleistocene to upper Pliocene	Prell et al., 1989
ODP Leg 117, Hole 728B	0.5-61m	Oman margin, water depth 1428m	Marly nannofossil ooze, carbonate content 50-65%	Pleistocene to upper Pliocene	Prell et al., 1989
ODP Leg 115, Hole 711A & B	A 2.5-5.3m B 4.4-18m	Mascarene Plateau, Indian Ocean. Water depth 4430m	Clayey nannofossil ooze, carbonate 40-60%	Pleistocene to upper Pliocene	Backman et al., (1988)
ODP Leg 115, Hole 709A	24-124m	Mascarene Plateau, Indian Ocean. Water depth 3038m	Clayey nannofossil ooze, carbonate 85-95%	Pleistocene to mid-Miocene	Backman et al., (1988)
Chalk	Outcrops	Isle of Wight and Sussex, U.K.	Chalk, carbonate >97%	Cretaceous (Campanian)	-
Lunde Formation sandstones, Cores 9/13a-36 and 9/13a-a45	3000-3300m 4300-4500m	northern North Sea, U.K.	Silty lacustrine sandstones	Late Triassic	Hounslow et al., (1995)
P-UK	Outcrops	Eastern England, U.K.	Clayey near-shore and marine sediments	early Pleistocene	-

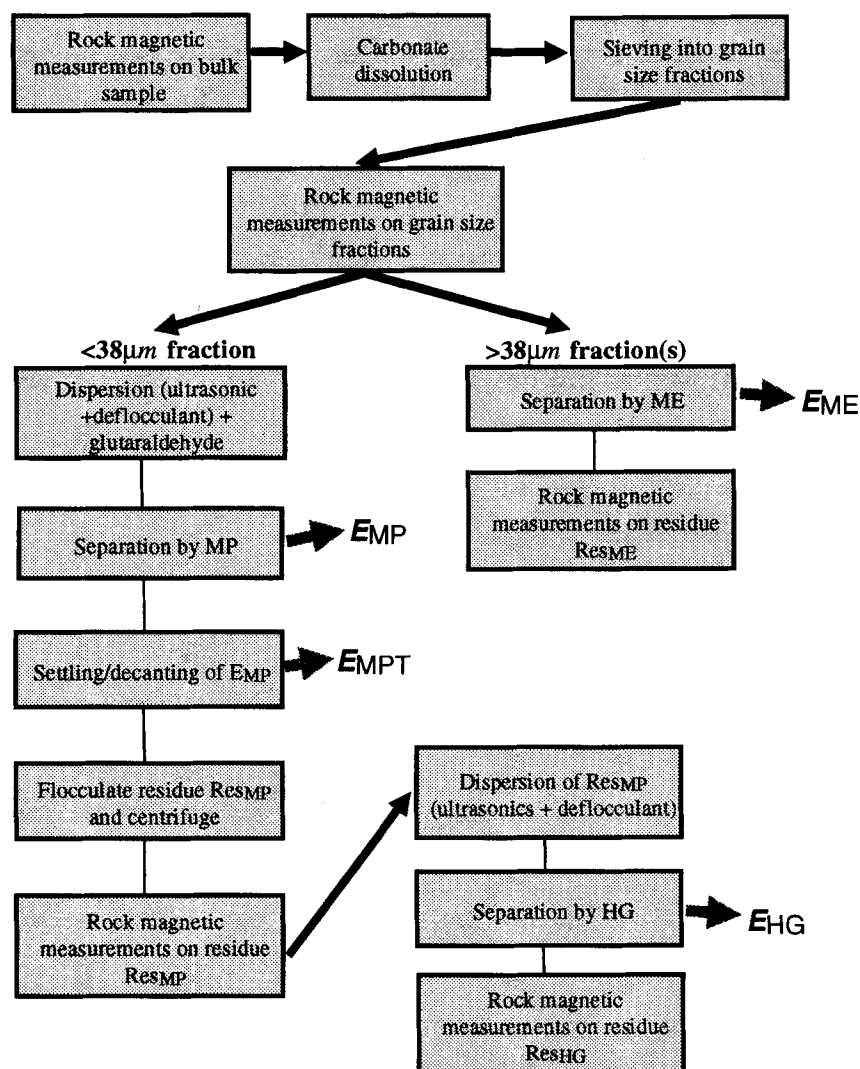


**Figure 1.** Outline of the procedure used in the extraction of magnetic minerals. MP = magnetized probe, ME = magnetic edge, HG = high gradient. See text for details.

depending upon the extraction objective and grain size of the sample (Fig. 1). The principal magnetic separation method used is the magnetized probe (MP) technique (Fig. 2 and Table 1). After carbonate removal, the sample is wet-sieved into two size fractions, one fraction coarser than  $38\ \mu\text{m}$ , the other finer than  $38\ \mu\text{m}$ . Only the  $<38\ \mu\text{m}$  fraction is used for MP separation since sand and coarse-grained silt cannot be kept in suspension and tend to block the flow system. The  $>38\ \mu\text{m}$  fraction was treated with the magnetic-edge (ME) separation procedure (see below).

Prior to any magnetic separation, the following rock magnetic measurements are undertaken on all sized fractions: susceptibility at  $0.46\ \text{kHz}$ , using a Bartington meter; anhysteretic remanence (ARM), imparted using a  $90\ \text{mT}$  of field in a dc field of  $0.08\ \text{mT}$ ; and isothermal remanences (IRM) at 20, 50, 100, 300 and  $1000\ \text{mT}$ , and measured using a MOLSPIN magnetometer. The susceptibility of ARM ( $\chi_{\text{ARM}}$ ) was also calculated, by normalizing the ARM with respect to the dc field used. Magnetic measurements at this stage also allow quantification of the relative importance of the various size fractions to the total magnetic properties.

#### *Magnetic extraction for grains $<38\ \mu\text{m}$*

In our procedure, the sample is dispersed (using Na-Hexametaphosphate, and ultrasonics) and circulated around the apparatus shown in Fig. 2 (Petersen *et al.* 1986), driven by a peristaltic pump (flow rate  $11\ \text{ml}\ \text{min}^{-1}$ ). Glutaraldehyde at 1 per cent v/v is added to stop any biological activity. The probe generates at its tip a magnetic field of  $\approx 40\ \text{mT}$ . The apparatus is run continuously for seven days, with collection of the extracted material once a day. Two extracts are produced: the main extract, flushed from the probe tip ( $E_{\text{MP}}$ ) using an extra distilled water reservoir; and an ultrafine extract ( $E_{\text{MPT}}$ ), which is collected from the often apparently clear water after settling of the main extract for three hours. The  $E_{\text{MPT}}$  extract is progressively collected over a seven-day period using a small supermagnet. These extracts are dried and weighed, to determine the weight per cent of the extract.

In addition to the magnetic extracts, this procedure produces two 'non-magnetic' residues,  $Res_{\text{MP}}$ , the main sample residue, and  $Res_{\text{MPT}}$ , the residue from the ultrafine, supernatant material.

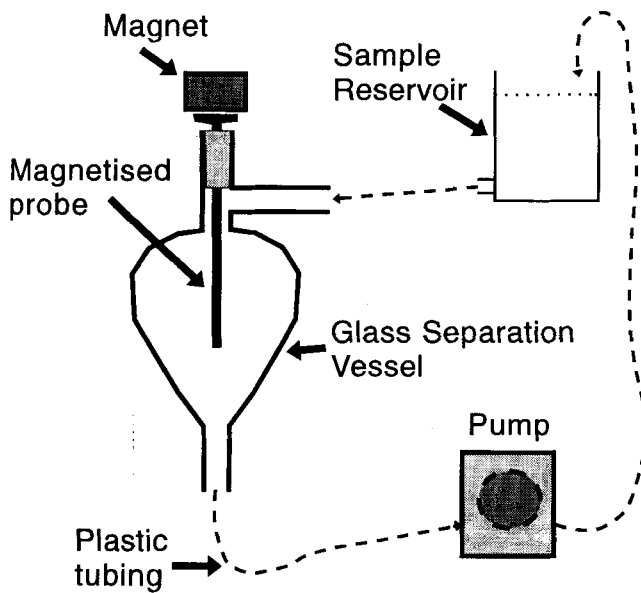


**Figure 2.** Schematic drawing (not to scale) of the magnetized probe magnetic extraction apparatus. The sample suspension is continuously circulated through the separation vessel. The magnetic extract collects on the magnetic probe tip and sides, as the suspension velocity reduces when it passes into the bulb of the vessel.

#### Magnetic extraction for grains $> 38 \mu\text{m}$

Those samples with abundant material coarser than  $38 \mu\text{m}$  were further subdivided by sieving, into a coarse silt fraction, and a very fine to fine sand fraction. For these fractions, magnetic extraction using magnetic edge (ME) separation is performed. A small rare-earth magnet (field  $\approx 0.3 \text{ T}$ ) is sealed in a polythene bag and suspended in an agitated suspension of the coarse grains. The magnetic separate is removed from the magnet edges to give extract  $E_{\text{ME}}$ . This extraction is repeated 10 times for each fraction, after which the extract is dried and weighed. The 'non-magnetic', coarse-fraction residues  $Res_{\text{ME}}$  result from this procedure.

#### Magnetic extraction of paramagnetic minerals

A further magnetic extraction can be performed on residue  $Res_{\text{MP}}$ , to examine the source of the paramagnetic susceptibility. We have performed this on some samples from the Indian Ocean, using the 'high gradient' (HG) separation technique, which produces extract  $E_{\text{HG}}$  (Fig. 1). A sealed perspex box (volume  $421 \text{ cm}^3$ ) filled with stainless steel wool is placed between the pole pieces of a  $0.8 \text{ T}$  electromagnet. A peristaltic pump passes a suspension of dispersed sample (in  $1.5 \text{ l}$ ) through the separator for  $1 \text{ h}$  at a flow rate of  $200 \text{ ml min}^{-1}$ . The extract  $E_{\text{HG}}$  is cleaned by first flushing the remaining sample from the separation box with distilled water. The extract  $E_{\text{HG}}$  is then removed from the box, concentrated by centrifuging, dried and weighed.

#### Quantification

The residues are recovered from suspension by using a concentrated  $\text{NaCl}$  solution to initiate flocculation, followed by centrifugation at  $4000 \text{ rpm}$  for  $15 \text{ min}$ . The rock magnetic

measurements conducted before extraction are repeated on the residues,  $Res_{\text{MP}}$ ,  $Res_{\text{ME}}$  and  $Res_{\text{HG}}$ , to determine what magnetic material has been left in the sample residues. From the before and after magnetic measurements, the amount of magnetic material removed is expressed as the extraction efficiency values,  $Eff_{\text{SUS}}$ ,  $Eff_{\text{SIRM}}$ ,  $Eff_{\text{ARM}}$ , for the susceptibility, SIRM ( $1 \text{ T}$ ), and ARM, respectively.

#### Identification of magnetic phases

There was normally sufficient magnetic extract in  $E_{\text{MP}}$ ,  $E_{\text{ME}}$  and  $E_{\text{HG}}$  for the major mineral phases to be identified by X-ray diffraction, using a Philips PW1710 with monochromatic Cu radiation, automatic divergence slit and scan speed  $0.005^\circ 2\theta \text{ s}^{-1}$ . This is accompanied by transmitted and reflected light optical microscopy (up to  $1000\times$  using oil immersion). The  $E_{\text{ME}}$  and  $E_{\text{MP}}$  extracts were also examined using scanning electron microscopy (Hitachi S450 with elemental dispersive X-ray analysis). The  $E_{\text{MPT}}$  extracts were examined by TEM (JEOL 100CX), with Link X-ray analysis facility, and, where appropriate, by selected area electron diffraction.

## RESULTS

### Extraction efficiencies

As can be seen from Table 3, the fine fractions ( $< 38 \mu\text{m}$ ) of the majority of our samples carry most of the magnetic signal; the ratio of the IRM in the fine fraction to that in the bulk sample IRM is often greater than 80 per cent. The exceptions are samples from ODP Hole 724C, the Lunde sandstones and the UK Pleistocene samples. Figs 3(a)–(c) show the extraction efficiencies of our modified MP procedure, with regard to susceptibility ( $Eff_{\text{SUS}}$ ), ARM ( $Eff_{\text{ARM}}$ ) and SIRM ( $Eff_{\text{SIRM}}$ ). The efficiencies vary but are notably high for a significant number of samples. For example, samples from Hole 709, Hole 722B and the Cretaceous chalk have  $Eff_{\text{ARM}}$  and  $Eff_{\text{SIRM}}$  values of between 60 and 95 per cent. When SIRM values exceed  $\approx 100 \times 10^{-5} \text{ A m}^2 \text{ kg}^{-1}$ , the relationship  $Eff_{\text{ARM}} > Eff_{\text{SIRM}} > Eff_{\text{SUS}}$  is common; otherwise,  $Eff_{\text{SIRM}}$  is generally larger than other extraction efficiencies. Some mineralogical bias results from the MP extraction process (Fig. 4); IRM measurements before and after extraction show that low coercivity material is preferentially extracted compared to the high-coercivity (e.g. haematite) component. However, in most samples, the bias is not severe, with an average 78 per cent of the 0–20 mT fraction extracted and 63 per cent of the 300–1000 mT fraction (Fig. 4). Haematite is not efficiently extracted when it dominates the magnetic properties, as in one of the Lunde sandstone samples ( $Eff_{\text{SIRM}} = 25$  per cent, Fig. 3(c) and the lowest data block in Fig. 4). Extraction efficiencies are also low for those sediments dominated by magnetic iron sulphides (one of the P-UK samples), with  $Eff_{\text{SIRM}}$  values of between 15 and 25 per cent (Fig. 3c).

Previously reported extraction efficiencies using the MP system (measured using low-field susceptibility) have generally been low. Bloemendal *et al.* (1993) reported an extraction efficiency of 30 per cent for the Hole 722B sediments; similarly, Verosub *et al.* (1994) describe problems with the MP system, obtaining only 50 per cent extraction efficiency and selective bias against the ultrafine ferrimagnetic fraction. Petersen *et al.*

**Table 3.** Rock magnetic parameters and extraction efficiencies for fine fractions (<38  $\mu\text{m}$ , after carbonate dissolution) used in MP magnetic extraction. Sample depths, or depth ranges, are shown for ODP cores.  $\text{IRM}_t/\text{IRM}_B$  per cent is the percentage of SIRM in this fraction to that in the bulk sample, and shows what proportion of the magnetizable material resides in this fraction.  $E_{\text{MP}}/\text{wt}_{\text{fine}}$  and  $E_{\text{MPT}}/\text{wt}_{\text{fine}}$  are the weight per cent of the extracts derived from the MP separation relative to that used in the MP extraction apparatus. [\* = <63  $\mu\text{m}$  fraction used in MP separation. — = not measured.

Sample	$\chi_{\text{ARM}}$	SIRM	$\frac{\text{IRM}_t}{\text{IRM}_B} \%$	weight%		$\chi_{\text{if}}$	Extraction efficiency	
	$\times 10^{-8}$ ( $\text{m}^3/\text{kg}$ )	$\times 10^{-5}$ ( $\text{Am}^2/\text{kg}$ )		$\frac{E_{\text{MP}}}{\text{wt}_{\text{fine}}}$	$\frac{E_{\text{MPT}}}{\text{wt}_{\text{fine}}} \times 10^{-3}$		ARM	SIRM
*722B (0.35m)	286	716	99.8	1.02	19.1	63	70	82
*722B (1.25m)	279	715	99.7	0.890	11.5	66	59	79
*722B (2.25m)	65.7	180	99.9	0.556	3.35	41	71	76
*722B (3.27m)	77.5	380	99.9	0.532	3.24	55	87	77
*722B (4.24m)	35.7	156	98.8	0.452	4.79	30	57	81
*722B (5.23m)	43.4	222	99.9	0.510	2.52	48	90	83
*722B (5.81m)	31.7	146	99.4	0.284	1.97	49	45	82
*722B (7.8m)	15.6	59.8	99.9	0.192	2.68	11	15	73
*722B (9.73m)	20.4	62.0	99.9	0.135	2.82	32	49	71
*722B (11.77m)	15.1	53.5	99.9	0.081	1.49	9	55	70
*722B (13.80m)	19.8	46.4	99.8	0.186	3.54	28	65	75
*722B (15.57m)	15.1	53.1	99.4	0.166	3.46	25	68	79
*722B (17.42m)	17.0	45.5	99.5	0.202	4.02	0	49	74
*722B (19.42m)	13.6	54.6	99.0	0.132	4.27	13	9	49
*722B (21.42m)	17.4	54.5	99.1	0.114	1.83	3	36	70
722B (1.87-6.47m)	37.7	280	91.9	0.100	5.03	62	59	86
722B (2.37-6.97m)	60.4	115	88.3	0.193	3.14	15	83	78
722B (26.8-29.0m)	11.9	35.1	65.3	0.245	1.95	13	18	60
722B (38.6m)	12.5	36.1	97.6	0.071	0.97	17	33	51
722B (40.6m)	13.1	36.7	96.3	0.111	0.86	10	7	54
722B (59.5-61.5m)	12.1	28.7	95.1	0.503	0.69	0	38	55
724C (0.33m)	22.0	87.3	23.1	0.265	0.19	34	0	59
724C (2.28-3.08m)	22.0	84.5	33.1	0.103	0.97	26	11	64
724C (19.5-22.0m)	19.9	53.2	29.5	0.109	1.71	20	-	-
724C (35.3-37.3m)	16.1	53.2	18.4	0.138	3.51	-	-	-
724C (47.1-49.1m)	19.5	50.8	9.0	0.089	0.39	22	-	-
728B (0.5-0.95m)	159	373	85.1	2.27	8.86	52	79	74
728B (1.45-2.4m)	15.6	130	97.9	0.176	0.78	39	40	81
728B (5.2-10.0m)	44.6	75.9	78.5	0.165	1.2	15	78	78
728B (58.6-61.0m)	21.7	45.0	63.8	0.010	0.38	13	67	59
709A (24.0-26.0m)	126	161	99.6	0.194	6.65	25	79	81
709A (28.0-29.7m)	28.7	63.1	99.5	0.145	4.51	31	81	80
709A (112.9m)	8.8	23.1	99.8	0.137	3.77	0	58	62
709A (118.4-120.4m)	1204	1026	100	0.280	13.58	44	74	67
709A (124.3m)	1137	1147	100	0.278	17.44	62	94	88
711B (4.4-6.4m)	794	703	99.5	0.196	11.39	27	39	45
711B (16.0-18.0m)	1050	863	99.9	0.172	4.5	33	51	44
711A (2.5-5.3m)	907	806	99.9	0.267	25.4	48	81	78
711 A (2.5-5.3m)	894	817	99.9	0.210	21.9	46	80	73
Chalk A	3.43	5.21	98.0	0.094	2.75	56	90	70
Chalk B	125.2	130	94.1	0.256	13.1	99	94	89
Chalk C	18.1	15.4	99.4	0.045	1.23	45	88	71
Lunde A	33.4	343	62.9	0.076	1.37	7	40	12
Lunde B	20.8	13.3	18.4	0.105	2.47	0	18	47
Lunde C	19.8	124.4	68.3	0.142	2.73	38	89	95
Lunde D	23.0	112.1	85.1	0.064	0.67	54	86	92
P-UK 1	48.4	293	89.6	-	-	50	88	37
P-UK 2	12.3	26.8	65.1	-	-	15	34	21
P-UK 3	10.1	19.5	86.5	-	-	64	62	54
P-UK 4	21.4	123	59.7	-	-	45	47	63
P-UK 5	19.6	145	0.4	-	-	15	10	14
P-UK 6	10.5	13.2	67.4	-	-	4	42	3
P-UK 7	8.01	9.97	56.6	-	-	0	37	21

(1986) report values of 30–40 per cent as typical for deep-sea sediments from the Angola Basin (DSDP Leg 73).

There is a negative relationship between the weight per cent recovered in the  $E_{\text{MP}}$  extract and the weight of sample from which the extraction was performed (Fig. 5). This might be

expected, since higher-density suspensions are more likely to suffer from physical interference between particles, with the result that weakly magnetic particles will be dislodged from the probe tip. However, the percentage extraction of initial susceptibility, ARM and SIRM shows no relationship with the

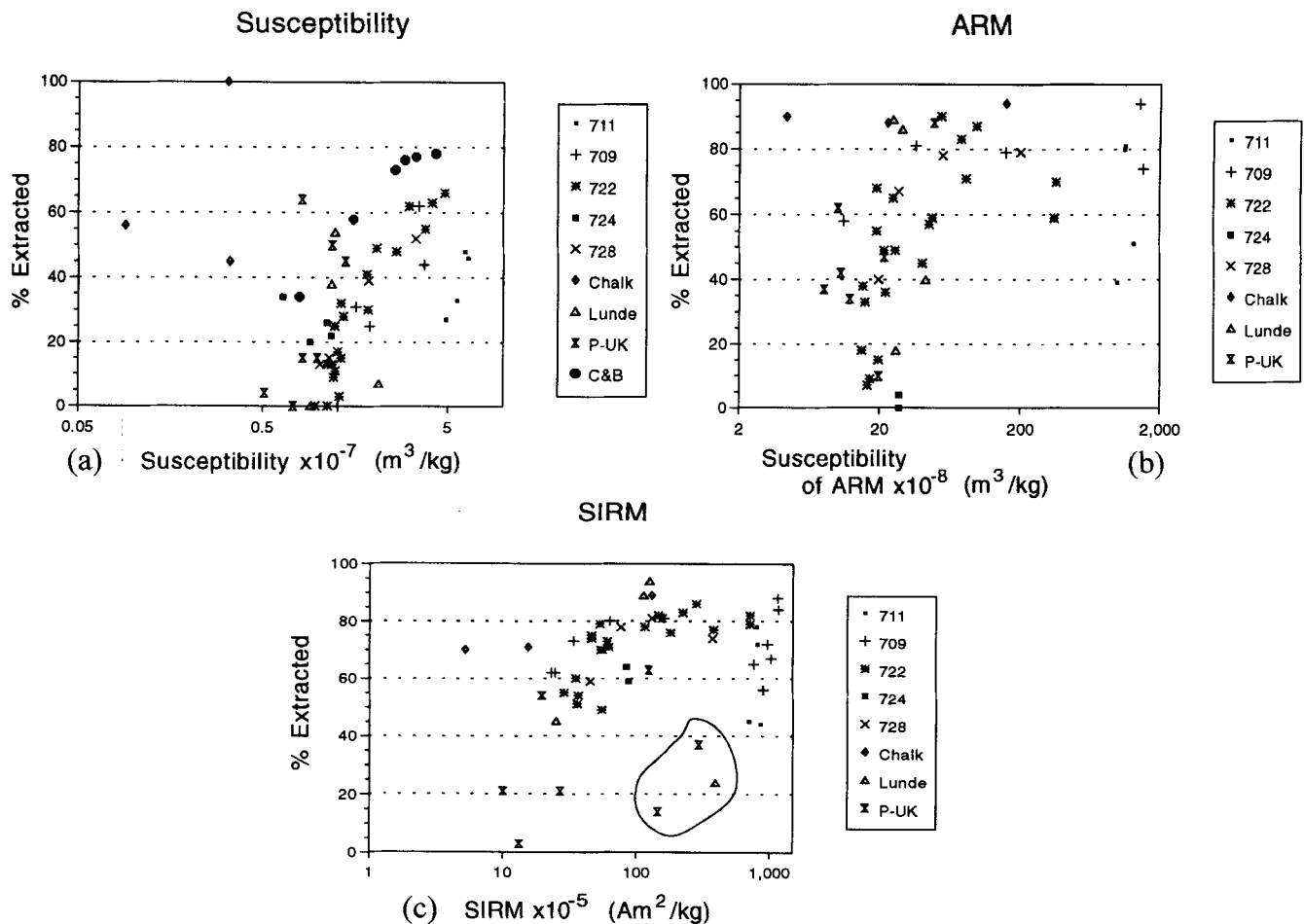


**Figure 3.** Extraction efficiencies of the MP separation, using three rock magnetic measurements: (a) initial susceptibility, (b) ARM and (c) SIRM (1 T). Note how the efficiency is related to the total amount of magnetic material present. In (a), 'C&B' are values for comparison from Canfield & Berner (1987) derived using an ME method of separation. In (c), the circled samples, which have  $Eff_{SIRM} < 40$  per cent and  $SIRM > 100 \times 10^{-5} \text{ A m}^2 \text{ kg}^{-1}$ , are dominated magnetically by haematite (one Lunde and one P-UK sample) or greigite (one P-UK sample).

weight of material used in the suspension. This suggests that the higher-density suspensions do not significantly modify the proportion of remanence-carrying material removed (see Discussion).

For the ME extraction system, the extraction efficiency from the  $>38 \mu\text{m}$  fractions, which in all but three sample suites carry a small contribution to the magnetic signal, tends to be rather variable, with  $Eff_{SIRM}$  generally larger than the susceptibility and ARM extraction efficiencies (Table 4). The values of  $Eff_{SIRM}$  and  $Eff_{SUS}$  are higher for those fractions possessing larger values of SIRM and susceptibility.

Applying the ME system to bulk sediment samples, Lovlie, Lowrie & Jacobs (1971) cite average  $Eff_{SUS}$  values of 70 per cent and  $Eff_{SIRM}$  of 50 per cent for pelagic oozes from the Aegean and the Indian Oceans, while Canfield & Berner (1987) measured  $Eff_{SUS}$  of 34–78 per cent on modern sediments (Fig. 3a).

The final stage of our sequential extraction procedure was to apply the HG method to the residue from the MP separation, in order to examine the source of the paramagnetic susceptibility (Fig. 1). We have applied this to selected samples from ODP Sites 709, 724, 728 and 722 in the Indian Ocean. Compared to the MP extraction, the HG procedure removes considerable amounts of material (weight per cent removed

8.3–28 per cent of  $Res_{MP}$ ; average, 22.2 per cent), with  $Eff_{SUS}$  values from 24 to 46 per cent (average 33 per cent). Additionally, HG extraction removes large proportions of the remaining ferrimagnetic grains in these samples ( $Eff_{SIRM}$ , 52–93 per cent; average, 74 per cent). A summary of the total amount of magnetic material removed at each extraction stage is shown in Fig. 6.

### Mineralogy of extracts

Not surprisingly, given the range of geological samples used here, the mineralogy of the extracts we obtained is quite diverse. Detailed discussion of these mineralogies will be made elsewhere, but here we focus on the broad groups of mineral relationships, and how and why these are represented in the magnetic extracts.

#### $E_{MPT}$ extracts

Transmission electron microscopy shows that the  $E_{MPT}$  extract concentrates the discrete grain submicron fraction, which may consist of bacterial magnetites, lithogenic magnetic particles and ultrafine, superparamagnetic-sized particles (Fig. 7). This is also borne out by the direct relationship between the

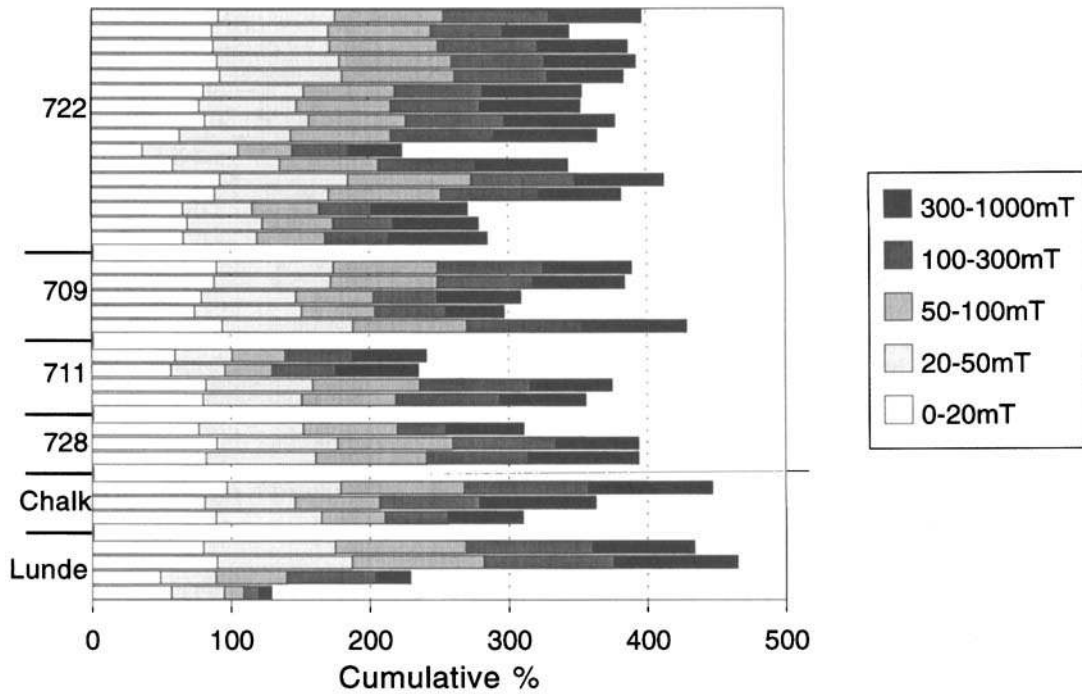


Figure 4. Percentage of IRM removed by MP separation, for five coercivity fractions. The length of the bar in each interval corresponds to the percentage removed, and total length of bar to the total SIRM removed in the extraction procedure (i.e. 100 per cent efficiency overall coercivity would give a cumulative percentage of 500).

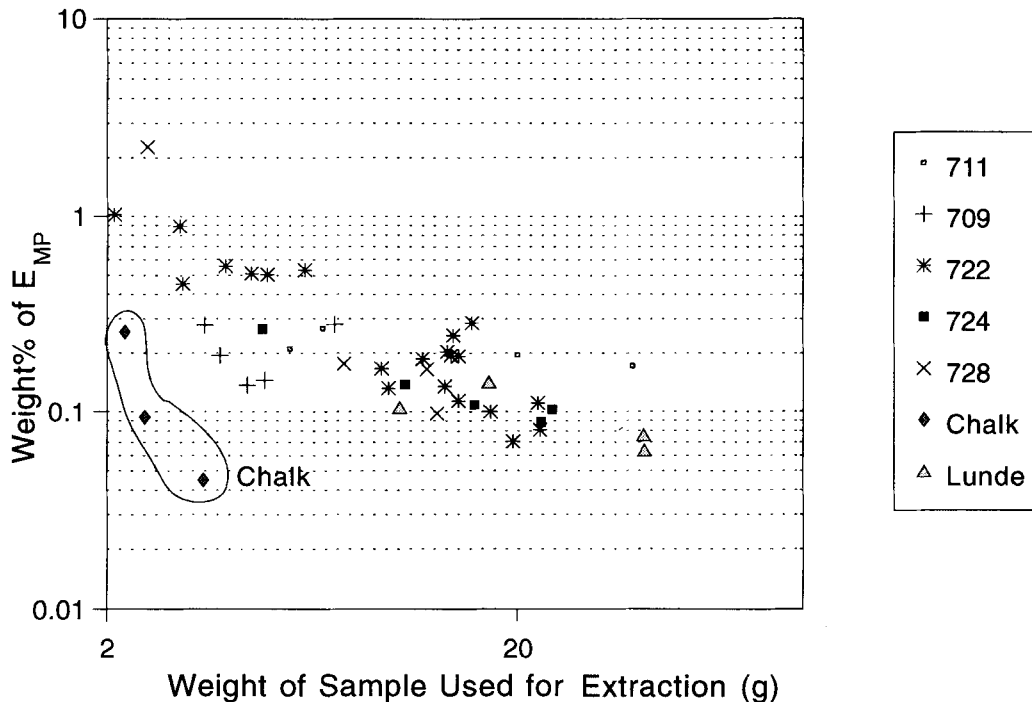


Figure 5. The weight per cent removed in the  $E_{MP}$  extract is inversely related to the total amount of material used in the MP extraction procedure. However, samples from the chalk (circled) do not follow the same trend. See text for details.

magnitude of the ARM and the weight per cent of the  $E_{MPT}$  extract (Fig. 8). Ferrimagnetic grains near the SP/SD boundary (i.e.  $\approx 0.03 \mu\text{m}$ ) acquire ARM most intensely (Ozdemir & Banerjee 1982; Maher 1988), and therefore would be expected to be concentrated into this extract.

Bacterial magnetosomes from the Cretaceous chalk appear

perfectly preserved (Fig. 7a), and show no apparent damage or dissolution effects from either the carbonate dissolution pre-treatment or the extraction process. Before- and after-extraction measurements of ARM (Fig. 3c) indicate an extraction efficiency of 90 per cent for these samples. Bloemendal *et al.* (1993) were unable to extract bacterial magnetosomes



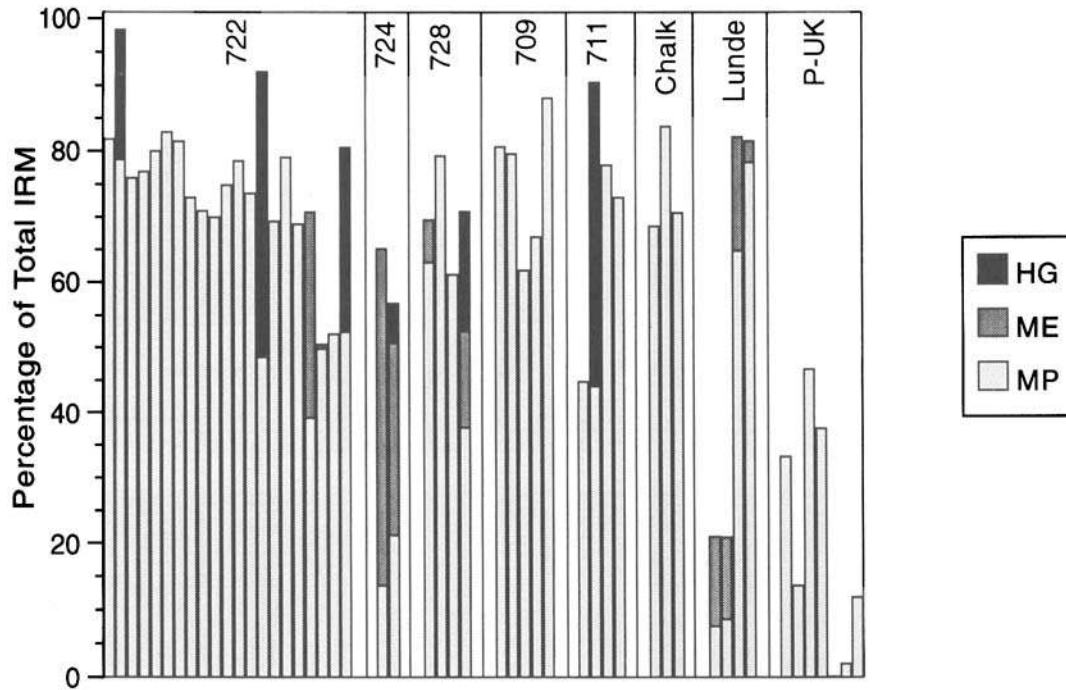


Figure 6. Percentage of IRM in the bulk sample removed by each of the three sequential separation methods. Coarse-fraction separations using the ME method were not generally performed on samples which have greater than 95 per cent of the IRM residing in the  $<38 \mu\text{m}$  fraction. HG extraction (using the residue  $Re_{MP}$ ) was only performed on selected samples.

from Hole 722B (despite using the MP system), which we have successfully extracted (Fig. 7b). This disparity may reflect the enhanced efficiency of the modified extract collection process. Bacterial magnetosomes are most concentrated in those samples with a weight per cent of  $E_{MPT}$  in excess of  $\approx 8 \times 10^{-3}$  per cent (Table 3). In contrast with the bacterial magnetosomes of Figs. 7(a) and (b), Fig. 7(c) shows the  $E_{MPT}$  extract from a Pleistocene palaeosol (palaeosol  $S_5$ ) from the Chinese Loess Plateau; the extract is rich in ultrafine-grained ferrimagnets, but not of direct bacterial origin. In the magnetite-dominated extracts, there is often a distinct compositional difference between larger grains ( $> \approx 0.1 \mu\text{m}$ ) and ultrafine grains ( $< 0.1 \mu\text{m}$ ), with the ultrafine grains lacking any substitution by titanium. Magnetite grains formed both by direct bacterial action (by magnetotactic bacteria) and indirectly (by bacterial reduction of iron, and subsequent chemical precipitation of magnetite) have been reported to be Ti-free (Walker *et al.* 1985; Maher & Taylor 1988).

The weight per cent of  $E_{MPT}$  is 10 to 100 times less than the weight per cent of the  $E_{MP}$  extract (Table 3). Samples with  $\chi_{ARM} > 200 \times 10^{-8} \text{ m}^3 \text{ kg}^{-1}$  have a larger  $E_{MPT}/E_{MP}$  weight ratio, reflecting the presence of proportionally more SP/SD material than in weaker samples.

The  $E_{MPT}$  extracts are generally similar in mineralogy to the  $E_{MP}$  extracts, except that they contain a higher ratio of ferrimagnetic to non-ferrimagnetic particles (Fig. 9). In those samples where the  $E_{MP}$  extract is dominated by diamagnetic silicates (e.g. most samples from ODP sites 722, 724, 728 and the Lunde samples), the  $E_{MPT}$  extracts generally contain diverse assemblages of silicates and Ti-oxide grains. However, it is unlikely that such grains occur due to inefficient magnetic separation, since any magnetic grains in the  $E_{MPT}$  have been through two magnetic concentration procedures. Their extraction is due either to the presence within them of magnetic inclusions, or

because they are strongly paramagnetic (Hounslow, Maher & Thistlewood 1995).

#### $E_{MP}$ extracts

For the fine-grained sediments (dominated by particles  $< 38 \mu\text{m}$ ), the  $E_{MP}$  extracts contain the bulk of the magnetically removed grains. The extracts contain diamagnetic, paramagnetic, antiferromagnetic and ferrimagnetic grains, depending upon the sample suite (Fig. 10). The Fe-Ti oxides, magnetite, haematite and ilmenite occur commonly in our range of samples (Figs 11a and d), whereas Fe-oxyhydroxides were not detected. Haematite seen under optical microscopy is commonly intergrown with detrital magnetite grains, which normally have a range of Ti-substitution. Ilmenite is particularly common in some samples (Fig. 10; samples from Holes 728B and 724C). Using SEM alone (i.e. without analysis by XRD), ilmenite could be mistaken for titanomagnetite, as neither morphology nor semi-quantitative elemental analysis may be diagnostic. Chromite and chromium-substituted magnetites are minor accessory phases in the extracts from some samples. The ferrimagnetic properties of three samples from the Lunde Formation are noteworthy, being dominated by ferrimagnetic Fe-substituted chromites and Mn-substituted magnetites (Fig. 11c; Hounslow *et al.* 1995). Freeman (1986) also found chromites abundant in extracts from some carbonate formations. Several of the UK Pleistocene samples dominantly contain ferrimagnetic iron sulphides; Fig. 7(d), for example, shows a sulphide-rich  $E_{ME}$  extract from one of these estuarine sediments. Their mineralogy probably lies within the greigite-pyrrhotite series (Hallam & Maher 1994).

Diamagnetic silicates, quartz and feldspars (plagioclase and K-feldspar; Fig. 11b) are common to all the extracts, often forming over 70 per cent of the extract. This is due to the

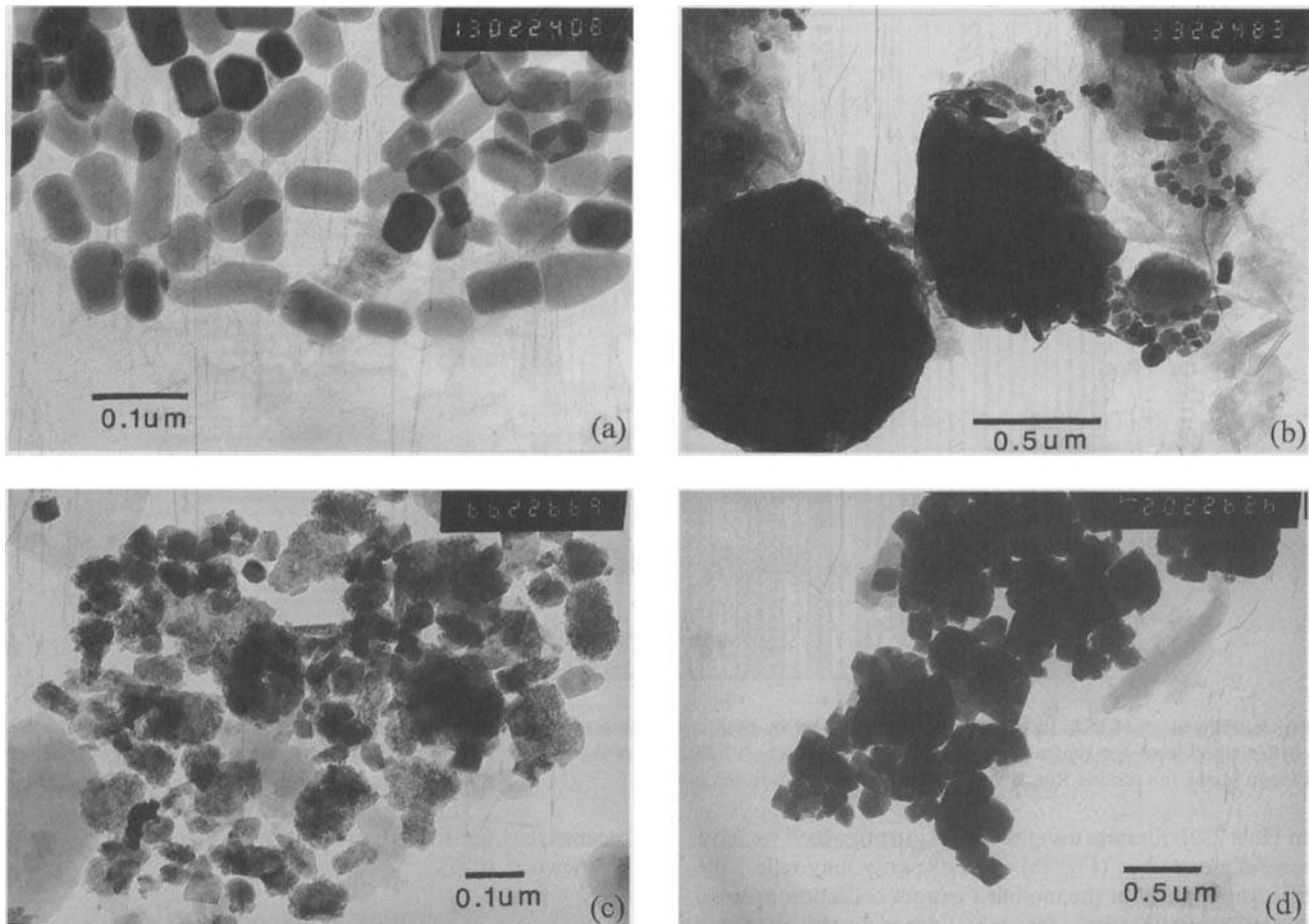


**Figure 7.** Transmission electron micrographs of (a) bacterial magnetosomes from the chalk, Culver Cliff, Isle of Wight. The magnetosomes appear well preserved in elongate chains, and are mostly prismatic but with a few equant and 'bullet'-shaped grains. (b) Large lithogenic magnetites and ultrafine bacterial chains of magnetite from the surficial sediments of Hole 722B (sample depth 1.25 m). The electron-transparent grains are silicates. (c) Pedogenic magnetites from Pleistocene palaeosol,  $S_5$  from Luochuan in the Chinese Loess Plateau. All the submicron particles are Ti-free, range in size from  $\sim 0.2$  to  $< 0.01 \mu\text{m}$ , and typically have ragged grain outlines, perhaps due to aggregation of SP particles or surface coatings of maghemite/haematite. (d) Iron sulphide grains (greigite?) from early Pleistocene estuarine sediments, East Anglia, UK, with typical rhomb-shaped grain outlines and well-defined edges, and a grain size of about  $0.7 \mu\text{m}$  to  $0.1 \mu\text{m}$ .

presence within these diamagnetic host grains of ferrimagnetic inclusions (Figs 12a and b). The presence of ferrimagnetic inclusions in feldspars, lithic fragments and volcanic glass has been reported previously (Evans & Wayman 1970; Morgan & Smith 1981; Geissmann *et al.* 1988; Vali *et al.* 1989; Heider, Korner & Bitschere 1993). The presence of such inclusions in quartz grains is less well known, but is prevalent in all the samples we investigated. The inclusions occur as visually observable, sometimes cubic, oxide grains (thought to be magnetic spinels), and as submicron clouds of grains which are barely observable in optical microscopy (i.e.  $< 0.1 \mu\text{m}$ ), but discolour the host grain. In reflected light, the internal reflections of these clouds are sometimes red, indicating the presence of some haematite. XRD also identifies kaolinite as a common, minor accessory phase, which is associated with altered feldspar grains. Such altered grains are abundant in extracts from the Pleistocene deep-sea samples from the Indian Ocean.

Other minerals, carrying no remanence, but common (if minor) in the extracts from the Pleistocene deep-sea sediments, are amphiboles, pyroxenes, chlorites, apatite, baryte and pyrite. Lovlie *et al.* (1971), Karlin & Levi (1985) and Canfield & Berner (1987) also found similar suites of paramagnetic

minerals. Some of these silicate minerals carry observable inclusions (Figs 12c, d and f), but many do not. We infer inclusions are present but submicron in size and difficult to locate and detect. Pyrite seems to be associated with sulphidized magnetites and ilmenites (Canfield & Berner 1987). In our pre-Pleistocene sediments, feldspars are significantly less abundant, and quartz often makes up a large proportion of the extracts. Rutile and anatase are also common in extracts from these older sediments (detrital, and associated with altered ilmenite), as too are micas, Mg–Cr-spinels, tourmaline and zircon, all of which may contain observable Fe-oxide inclusions (Fig. 12e).

#### *E<sub>ME</sub>* extracts

The ME extraction produces a similar weight per cent of material to that from the MP magnetic separation (Table 4). For some coarser-grained, silt and fine sand-dominated sediments (e.g. Hole 724C, Lunde samples), more than 80 per cent of both the total SIRM and ARM reside in the  $> 38 \mu\text{m}$  fraction (Table 4; Hounslow *et al.* 1995), indicating the signifi-

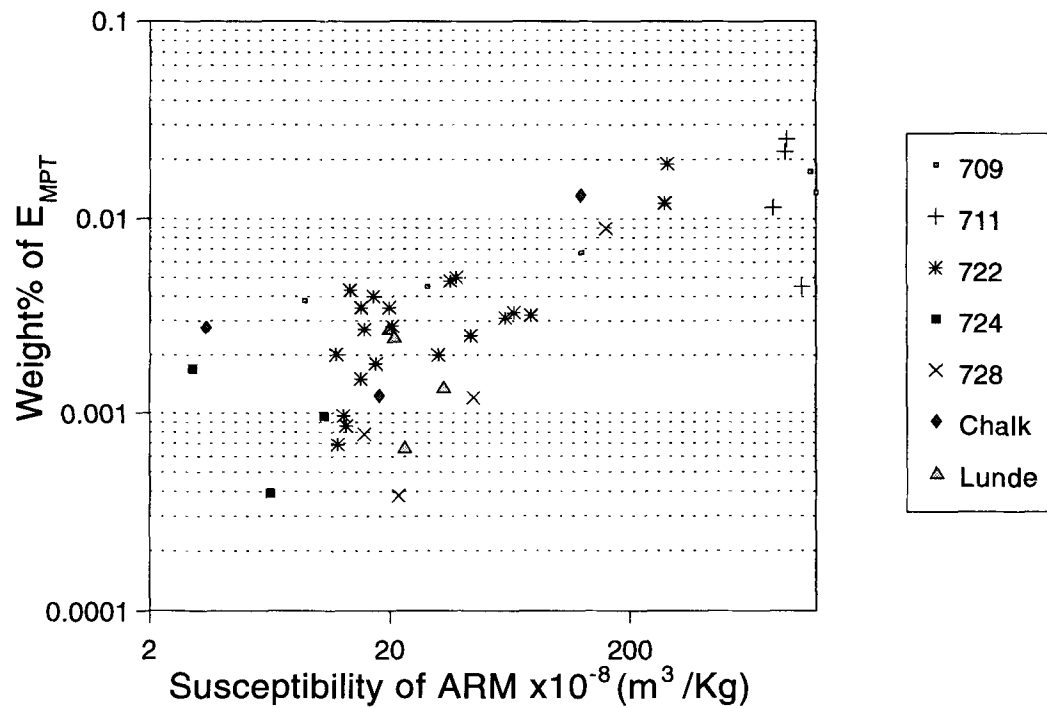


Figure 8. The weight per cent of the  $E_{MPT}$  extract is approximately proportional to the abundance of fine-grained, SP/SD material as measured by the susceptibility of ARM.

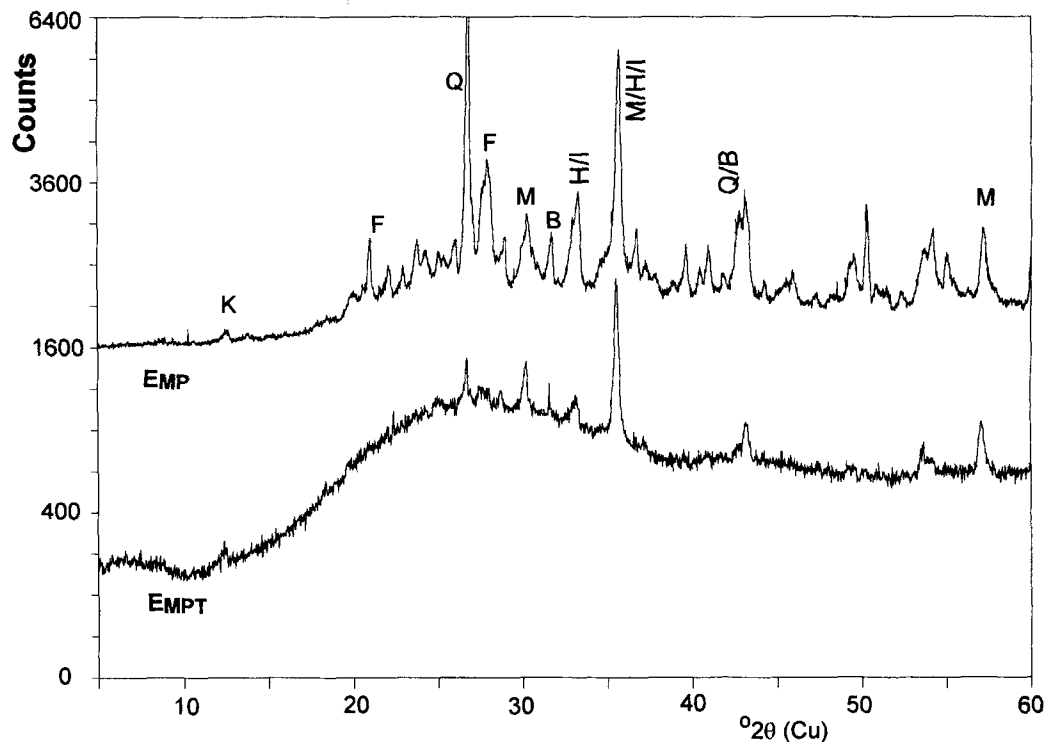
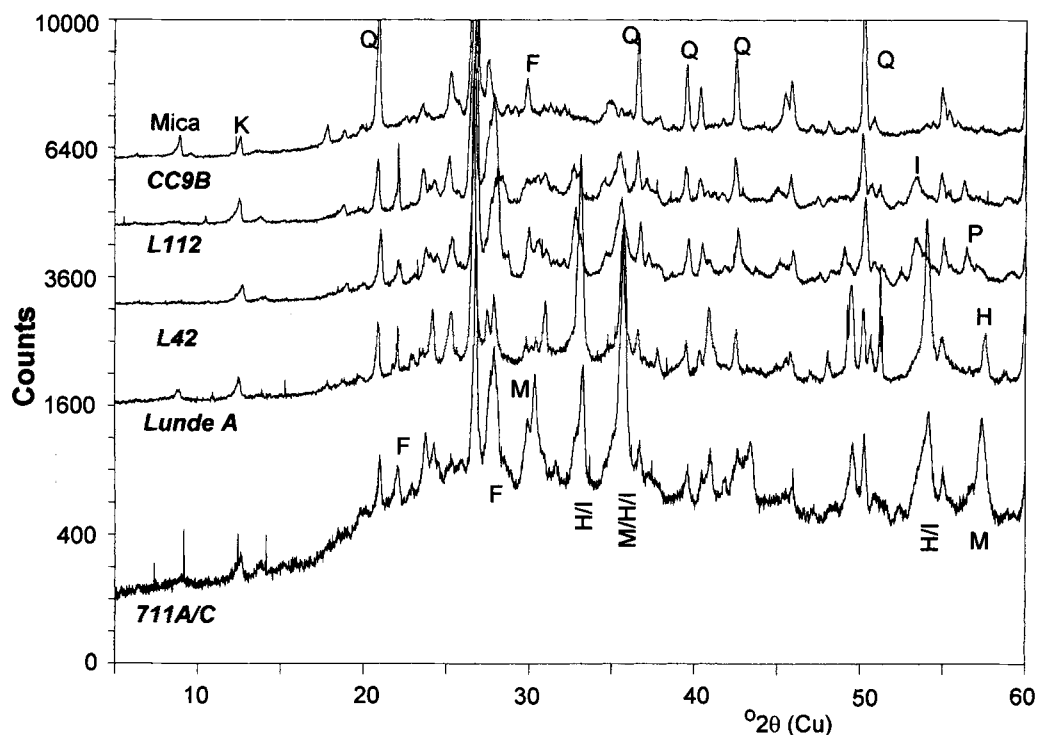


Figure 9. X-ray diffraction data for the  $E_{MP}$  and  $E_{MPT}$  extracts for a sample from ODP site 709A (sample depth 119 m). The  $E_{MP}$  extract has approximately equal proportions of quartz, feldspar and magnetite, with smaller amounts of haematite, baryte and kaolin. The  $E_{MPT}$  extract is depleted in quartz and feldspar, and enriched in magnetite. K = kaolin or chlorite; F = plagioclase feldspar, Q = quartz, M = magnetite, B = baryte, H = haematite, I = ilmenite.

cance of this fraction in controlling the ferrimagnetic properties in some cases.

Compared to the  $E_{MP}$  extracts, the  $E_{ME}$  extracts contain larger amounts of strongly paramagnetic minerals, such as

pyroxenes, amphiboles, chlorites, micas, Mg–Cr-spinels, garnets, Ti-oxides, apatites, tourmaline, zircon, Fe-carbonates and other accessory grains (amphiboles and pyroxenes are only found in extracts from the Indian Ocean samples). These occur



**Figure 10.** Selected X-ray diffraction data from the  $E_{MP}$  extracts, showing the presence of significant amounts of extracted silicate minerals. K = kaolin or chlorite, Q = quartz, F = feldspar, H = haematite, I = ilmenite, M = magnetite, P = pyrite. 711A/C = Hole 711A (sample depth 2.4–5.2 m), mostly feldspar, magnetite and quartz, smaller amounts of ilmenite, haematite, baryte and kaolin. Lunde A is dominated by haematite and quartz, with smaller amounts of ilmenite, feldspar, rutile, kaolin/chlorite and mica. L42 = Hole 722B (sample depth 7.8 m), mostly quartz, feldspar and ilmenite, smaller amounts of pyrite, magnetite, haematite and kaolin/chlorite. L112 = Hole 724C (sample depth 36 m), feldspar and quartz, smaller amounts of ilmenite, pyrite, magnetite, rutile and kaolin. CC9B = chalk from Culver Cliff, Isle of Wight, quartz and orthoclase feldspar, with mica, chlorite, anatase, and no XRD-detectable magnetite.

in addition to inclusion-containing quartz and feldspar grains, and more strongly magnetic Fe–Ti and Cr oxides (Figs 11d and 12c). Also found in some of the ODP site 709 and 711 carbonate-rich, deep-sea sediments are cosmic spherules, particularly abundant in  $E_{ME}$ , but also present in minor amounts in the  $E_{MP}$  extracts. The relative amounts of paramagnetic minerals vary greatly between different sample suites, reflecting the diverse provenance of these minerals.

#### $E_{HG}$ extracts

The  $E_{HG}$  extracts are dominated by clay minerals, with smaller amounts of quartz. The dominant clay minerals in our extracts are chlorites, micas and kaolinites with smaller amounts of smectites (Fig. 13), along with a variety of accessory paramagnetic minerals. The residue from the HG extraction tends to be paler coloured than the original sediment, attesting to the efficiency of the process in removing Fe-bearing clays. However, the  $Eff_{sus}$  values are typically about 30 per cent and the amount of material removed is large, showing that the paramagnetic susceptibility of these sediments is carried by abundant, weakly magnetic terrigenous clay minerals.

## DISCUSSION

Application of an efficient and quantitative procedure for magnetic mineral extraction may (a) enable quantification of

the amounts and origins of magnetic minerals in natural samples; (b) assist the ongoing development of rock magnetic measurements and parameters which characterize grains from specific origins (e.g. Jackson *et al.* 1993; Oldfield 1994); and (c) identify whether the magnetic grains extracted are representative, and their contribution to the rock magnetic or palaeomagnetic signal.

One of the major features of the data obtained here is the diverse and complex nature of the mineralogies extracted. Magnetic particles cannot be considered in isolation from the grains which constitute most of the host rock, since both magnetic and non-magnetic suites often share a common origin. The remanence-carrying minerals can be categorized into two classes of mineral associations.

(1) Discrete particles, such as detrital magnetite, haematite or ferrian chromite grains (Figs 11a, c and d), individual bacterial magnetosomes (Fig. 7a), or diagenetic sulphide particles (Fig. 7d). These particles are normally presumed to carry the NRM and rock magnetic properties.

(2) Particles as inclusions in non-remanence-carrying host grains, which may be diamagnetic, paramagnetic or multicomponent volcanic glass and rock fragments. These inclusions have the potential to be significant in rock magnetic studies, and also to carry the NRM in some cases, especially where discrete ferrimagnetic grains are lacking (Heider *et al.* 1993; Hounslow *et al.* 1995).

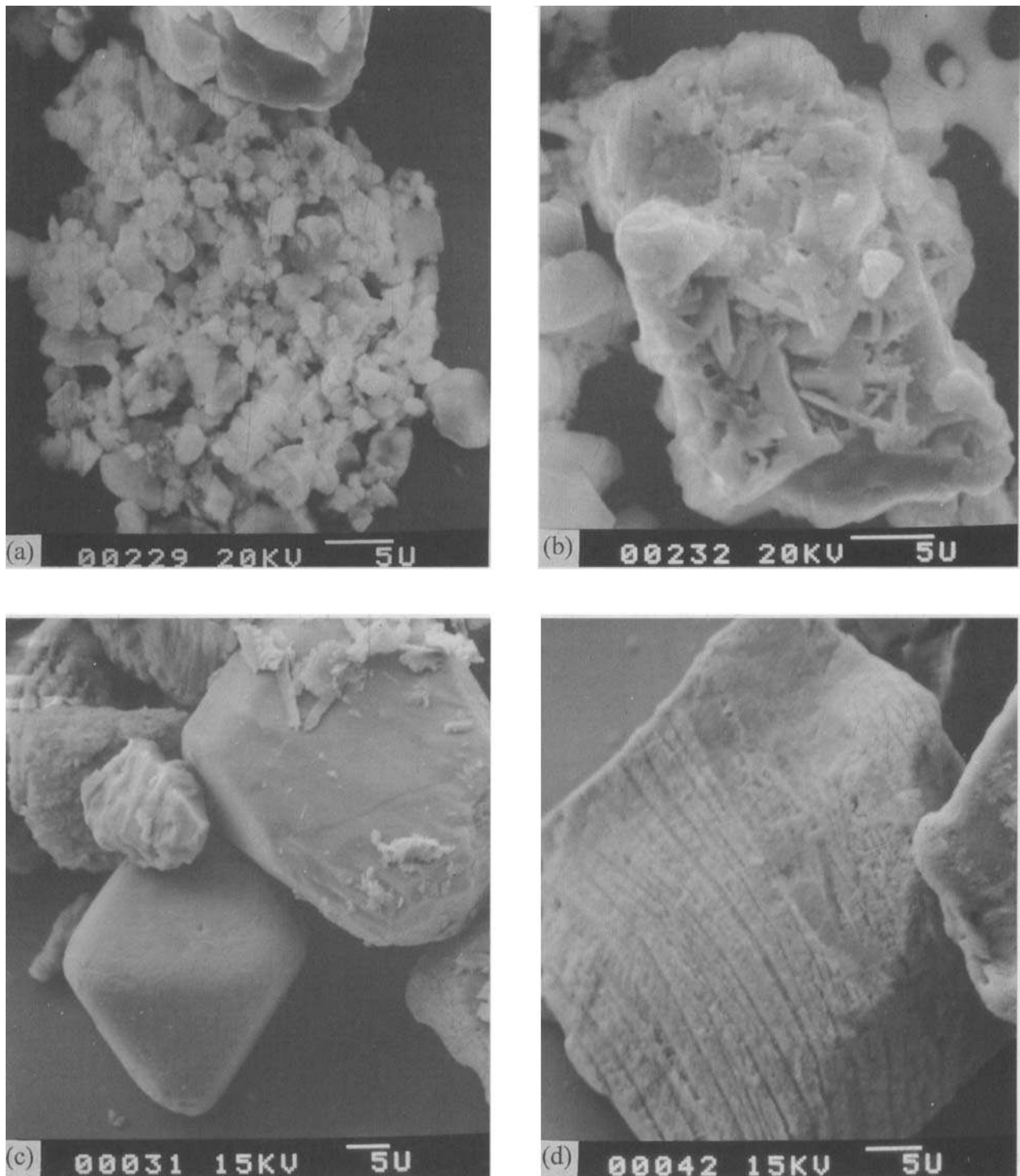


**Figure 11.** SEM micrographs of strongly magnetic mineral grains from  $E_{MP}$  extracts. (a) Hole 709A (sample depth 4.5–6 m), a clump of strongly magnetic detrital Fe–Ti oxides, mostly less than 2  $\mu\text{m}$  in size. (b) Hole 709A (sample depth 4.5–6 m) Ca-feldspar rich in Fe with needles of magnetite or haematite protruding from the surface. (c) Lunde sample B, variously shaped chromite grains, the lower one an abraded octahedral grain. (d) Lunde sample A ( $E_{ME}$  extract), an ilmeno-haematite grain, with the darker regions rich in ilmenite and the pale regions rich in haematite.

The efficiency of extraction of the magnetic minerals from any sediment will depend not only upon the equipment used, but also on the magnetic mineralogy, composition and intergrowth relationships. Given a population of sample grains spanning the submicron to silt-size range, varying in mineralogy, and varying in structure (e.g. discrete grains, inclusions,

intergrowths), we might view the MP extraction process as a series of statistical opportunities for trapping of 'magnetic' grains. For those particles occurring as magnetic inclusions within diamagnetic host grains, the magnetic moment of the inclusions has to counteract diamagnetic repulsion from the field gradient. A discrete particle will have a larger net attrac-

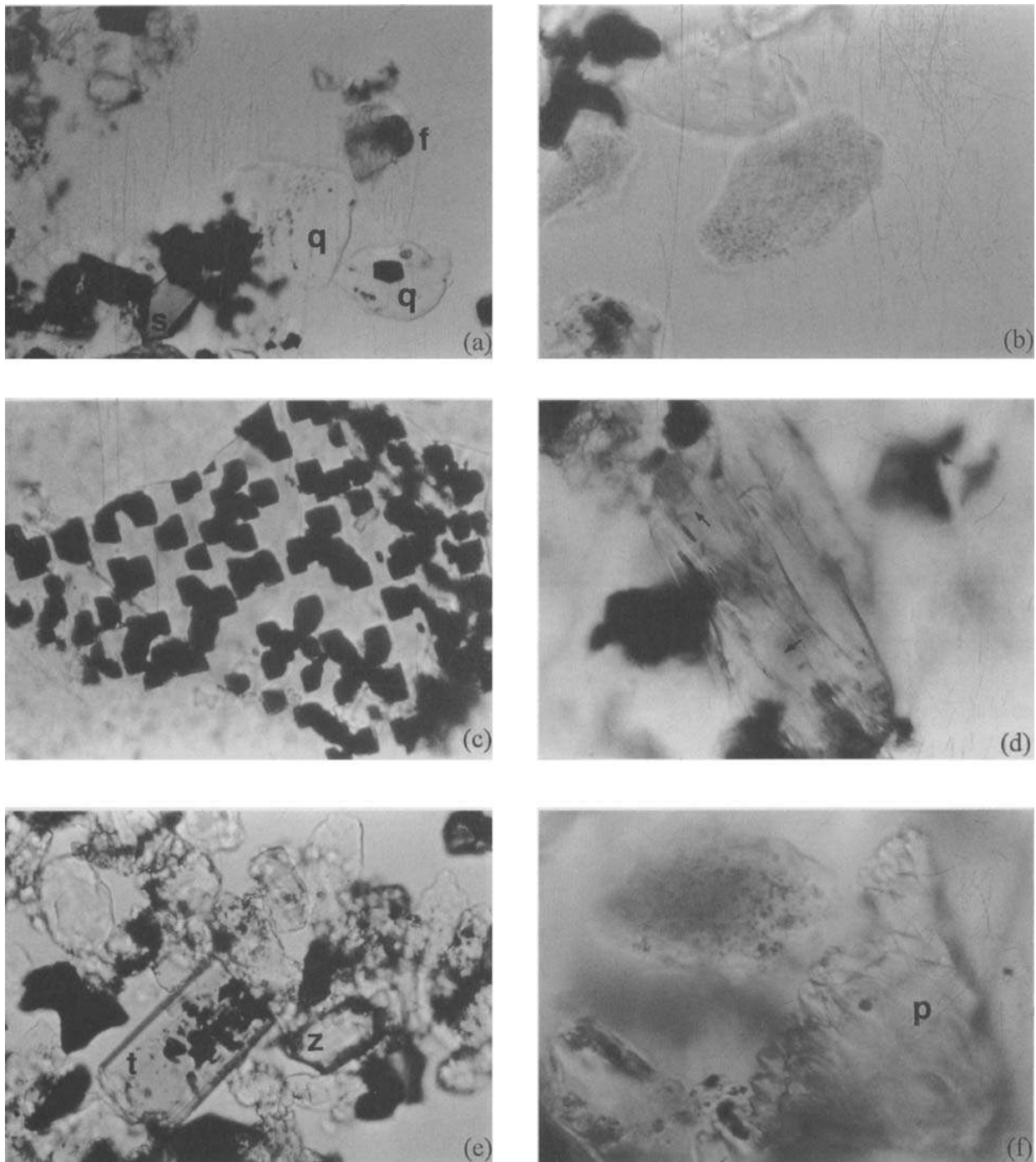


**Figure 12.** Optical micrographs from  $E_{MP}$  extracts. (a) Hole 722B (sample depth 5.8 m): many quartz grains (q) with inclusions of various sizes, a cloudy feldspar (f) grain and brown picotite spinel (s) (width of micrograph = 155  $\mu\text{m}$ ). (b) Hole 722B (sample depth 5.8 m): heavily clouded feldspar with many submicron inclusions, which are red (haematite) in reflected light (width of micrograph = 60  $\mu\text{m}$ ). (c) Hole 709A  $E_{ME}$  extract (sample depth 4.4–5.9 m): a chlorite grain crowded with Fe-oxide octahedra and dendrites (width of micrograph = 155  $\mu\text{m}$ ). (d) Hole 722B (sample depth 5.2 m): hornblende fragment with elongate Fe-oxide inclusions aligned in two perpendicular directions (width of micrograph = 155  $\mu\text{m}$ ). (e) Lunde sample D: Fe-oxide inclusions in a tourmaline grain (t), with an adjacent zircon (z). Many surrounding quartz grains have abundant Fe-oxide inclusions (width of micrograph = 155  $\mu\text{m}$ ). (f) Hole 722B (sample depth 11.8 m): etched pyroxene grain (p) with opaque inclusion (width of micrograph = 60  $\mu\text{m}$ ).

tion than the same-sized particle included in a diamagnetic grain. Consequently, samples dominated by discrete magnetic particles will have higher extraction efficiencies than those dominated by inclusion mineralogies. Similar reasoning also applies to the ME extraction process. We believe this to be

the major cause of the variation in extraction percentages between samples, as shown in Fig. 3 and Table 4. Extraction efficiencies tend to be higher for samples with higher magnetization values (which have more discrete magnetic grains), and lower for those samples with more abundant inclusions. This

**Table 4.** Rock magnetic parameters and extraction efficiencies for  $E_{ME}$  extractions from the coarse fractions. Sample depths, or depth ranges, in the cores from the ODP samples are shown. Lunde samples have virtually no grains larger than 250  $\mu\text{m}$ .  $IRM_c/IRM_B$  per cent and  $ARM_c/ARM_B$  per cent are the percentage of the SIRM and ARM of the coarse fraction, to that in the bulk sample.  $E_{ME}/wt_{coarse}$  is the weight per cent of the extract derived from the ME separation relative to that used in the ME extraction. — = not measured.

Sample (grain size)	SIRM $\times 10^{-5}$ ( $\text{Am}^2/\text{kg}$ )	$\frac{IRM_c}{IRM_B}$ %	$\frac{ARM_c}{ARM_B}$ %	weight% $\frac{E_{ME}}{wt_{coarse}}$	Extraction efficiency		
					$\chi_{if}$	ARM	SIRM
Lunde A (38-63 $\mu\text{m}$ )	170.5	16.0	14	0.138	29	10	22
Lunde A (64-250 $\mu\text{m}$ )	67.1	21.8	28	0.312	48	55	48
Lunde B (38-63 $\mu\text{m}$ )	13.1	23.7	20	0.173	35	13	35
Lunde B (64-250 $\mu\text{m}$ )	7.0	56.8	62	0.033	48	33	7
Lunde C (38-63 $\mu\text{m}$ )	17.8	7.1	8.9	1.05	36	37	66
Lunde C (64-250 $\mu\text{m}$ )	8.6	24.1	34	0.208	75	21	52
Lunde D (38-63 $\mu\text{m}$ )	14.0	6.0	11	0.470	12	0	31
Lunde D (64-250 $\mu\text{m}$ )	8.9	8.9	21	0.180	7	5	15
722B, 26.8-29m (>38 $\mu\text{m}$ )	189.9	34.7	5.9	0.339	71	44	91
722B, 38.6m (>38 $\mu\text{m}$ )	29.6	2.4	0.21	0.342	30	-	25
724C, 0.33m (>38 $\mu\text{m}$ )	102.4	76.9	98	0.114	26	27	67
724C, 2.28-3.08m (>38 $\mu\text{m}$ )	101.2	66.9	79	0.422	31	14	44
724C, 19.5-22.0m (>38 $\mu\text{m}$ )	86.2	70.5	94	0.421	30	43	40
724C, 35.3-37.3m (>38 $\mu\text{m}$ )	73.8	81.6	98	0.412	30	13	38
724C, 47.1-49.1m (>38 $\mu\text{m}$ )	90.2	91.0	84	0.288	27	29	40
728B (5.2-10m) (>38 $\mu\text{m}$ )	62.5	21.5	-	0.423	42	-	44
728B (58.6-61m) (>38 $\mu\text{m}$ )	64.5	36.2	98	0.586	27	19	41

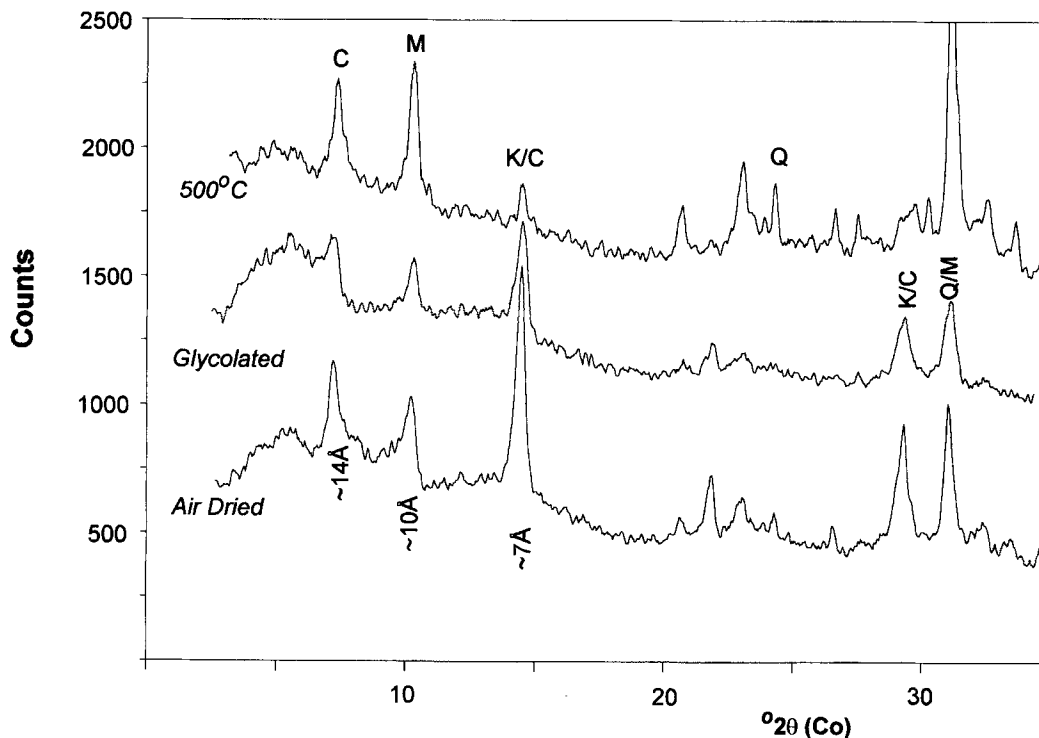


**Figure 13.** X-ray diffraction data for HG extract from Hole 115-709A (4.5-6 m depth). XRD traces are shown for the untreated, glycolated and 500°C treated sample, which allow determination of the mineralogy of the extract. This sample consists mostly of clay minerals, micas (M), chlorite (C) and kaolin (K), with quartz (Q) and small amounts of feldspar. The broad peak at  $\sim 5^\circ$  ( $2\theta$ ) is due to opal from siliceous microfossils.

is borne out by XRD analysis of the mineralogy of the extracts; those extracts poor in ferrimagnetic spinel minerals have lower overall extraction percentages. Those samples ( $< 38 \mu\text{m}$ ) with  $\chi_{ARM}$  values of about  $20 \times 10^{-5} \text{ m}^3 \text{ kg}^{-1}$  (Fig. 2b) have few discrete submicron magnetic particles and abundant silicates with inclusions. Hence, we infer their magnetization is largely carried by particles as inclusions (possibly of a wide grain-size

range), which are not efficiently removed by MP extraction. Susceptibility values, as shown in Fig. 3(a), are contributed to by a combination of paramagnetic and ferrimagnetic minerals. Those samples with susceptibilities less than  $\approx 2 \times 10^{-7} \text{ m}^3 \text{ kg}^{-1}$  are dominated by paramagnetism. These paramagnet-dominated samples have low-susceptibility extraction efficiencies because the MP separation uses a relatively



small magnetic field ( $\approx 40$  mT) and thereby preferentially concentrates ferrimagnets.

Another factor is also at play here—that of sample suspension density, which will determine the amount of grain interaction at the probe tip. At low suspension densities (i.e. small initial sample weight; Fig. 5), physical grain interaction will be less, and grains with a low net attraction to the probe tip will have a better chance of becoming attached. The converse is true for high-density suspensions (large sample weight; Fig. 5). For inclusions, the size of the host diamagnetic or paramagnetic grain also has a significant control; a small host grain has more chance of attaching to the probe tip than a larger host grain with the same ferrimagnetic inclusion. This effect is shown by the chalk samples, in which the quartz grains are predominantly fine-silt in size, whereas our other samples are predominantly medium silt-sized. The chalk samples have high SIRM and ARM extraction efficiencies, yet the  $E_{MP}$  extract is dominated by diamagnetic silicates with inclusions.

From the relationship in Fig. 5, it might be expected that extraction efficiency could be increased by using small amounts of parent sample, producing low-density suspensions, least physical interaction between particles, and maximum trapping opportunity. However, the extraction process should ideally produce enough extract for analysis by XRD and microscopy. In addition, low sample concentrations are more prone to environmental contamination, and possible loss of fine-grained material if flocculation density is low. Therefore, there is a trade-off between maximizing extraction opportunity on the one hand, and obtaining sufficient and representative extracted material on the other.

The particular separation equipment used should match the task in hand. HG magnetic separation is best suited for removing paramagnetic minerals, which in some samples may be significant in controlling the susceptibility. If this method

is used on the bulk sample, the ferrimagnetic grains will likely be removed efficiently, but they will be mixed with far more abundant paramagnetic minerals, therefore making isolation and identification of fine-grained ferrimagnetic particles difficult. MP magnetic separation is best suited for concentrating the ultrafine and silt-sized ferrimagnetic spinel fraction, but does not fare well at removing haematite, goethite and some magnetic sulphides. ME magnetic separation will be less effective at removing ultrafine ferrimagnetic phases, particularly if flow rates are high and extraction duration short (Von Dobeneck 1985). However, this method is good at extracting larger ferrimagnets and the stronger paramagnetic phases.

It has been suggested by Sun & Jackson (1994) that the carbonate dissolution pre-treatment, using buffered acetic acid, dissolves significant amounts ( $\approx 60$  per cent) of the ultrafine-grained Fe-oxides. We have found no evidence for this. First, we have extracted bacterial magnetite which shows no evidence of dissolution (Fig. 7a), despite using much stronger acid concentrations. Second, we determined rock magnetic properties of the non-carbonate fraction before and after carbonate dissolution (carbonate abundance determined using X-ray fluorescence data). Since ARM is particularly sensitive to the presence of magnetite grains  $\approx 0.03 \mu\text{m}$  in size, it should reflect any ferrimagnetic dissolution strongly, yet data are in approximate agreement before and after dissolution (Fig. 14). The large amount of scatter seen in Fig. 14 can probably be accounted for by inhomogeneity between the measured subsample and the parent bulk sample used for dissolution. Similar, non-systematic scatter exists for the SIRM and coercivity fraction data, before and after carbonate dissolution. The differing conclusions reached here and by Sun & Jackson (1994) may be due to the procedure during carbonate dissolution. Sun & Jackson (1994) changed the acid approximately 30 times over a six-week period, whereas we used up to only

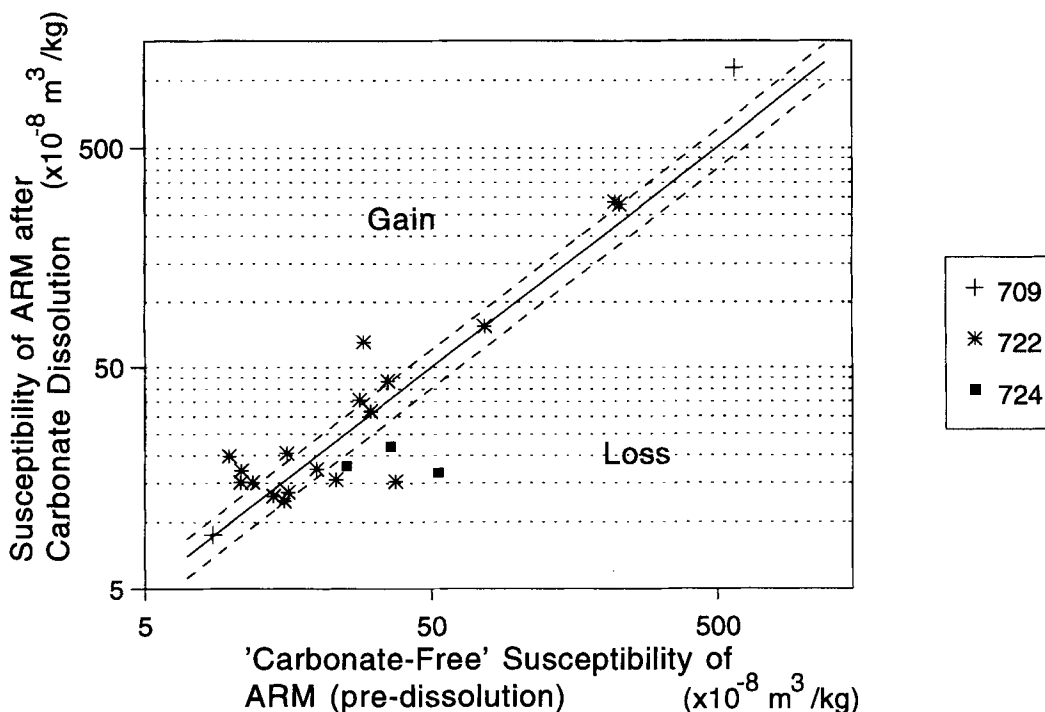


Figure 14.  $\chi_{ARM}$  of the non-carbonate fraction before and after dissolution of the carbonate with acetic acid. The amount of carbonate was determined by XRF, and measured whole-rock ARM adjusted accordingly. The  $\pm 20$  per cent bars are drawn parallel to the 1:1 correlation line.



four changes. During the process of removal of the exhausted acid, there is uncertainty as to how much sample is thrown away in the apparently clear solution, unless it is centrifuged. The likelihood of significant loss increases as more acid changes take place.

## CONCLUSIONS

(1) Quantification of magnetic extraction procedures and improved extraction efficiency enable the abundance of magnetic minerals from various sources to be estimated, when combined with microscopy and X-ray diffraction. In turn, this will promote the characterization of magnetic mineral sources using rock magnetic measurements.

(2) Extraction efficiencies, calculated in terms of low-field susceptibility, anhysteretic remanence and IRM, vary depending upon the mineral source of these properties and also the mineral intergrowth relationships with diamagnetic and paramagnetic minerals. Using the MP system on the <38  $\mu\text{m}$  size fractions, IRM and ARM extraction efficiencies are commonly in excess of 70 per cent for strongly magnetic samples ( $\text{SIRM} > 80 \times 10^{-5} \text{ A m}^2 \text{ kg}^{-1}$ ). Where the remanence properties are dominated by haematite or iron sulphides, extraction efficiencies are significantly lower (<25 per cent). Susceptibility extraction efficiencies are strongly influenced by whether the susceptibility is of a paramagnetic or ferrimagnetic origin.

(3) Our extraction procedure produces potentially four magnetic extracts: (a) an ultrafine fraction, suitable for TEM analysis; (b) a silt-sized fraction ( $\sim 2\text{--}38 \mu\text{m}$ ); (c) a coarse-silt and sand-sized fraction; and (d) a paramagnetic clay fraction. The ultrafine fraction concentrates discrete SP and SD ferrimagnetic particles such as bacterial magnetosomes. The silt and sand fractions concentrate the lithogenic remanence-carrying magnetic minerals such as ferrimagnetic spinels (Ti-magnetites, ferrian chromites), ferrimagnetic sulphides and haematites. Various paramagnetic minerals are also significant accessory phases in all samples, but especially in the  $E_{\text{HG}}$  extract.

(4) Applying these methods to a range of sediments, we have found that ferrimagnetic minerals are present in two forms: (a) discrete particles from  $\approx 0.01 \mu\text{m}$  to  $\approx 100 \mu\text{m}$  in size, not significantly intergrown with other minerals; and (b) inclusions within diamagnetic (principally quartz and feldspar) and paramagnetic silicates, which we infer to have a similar ferrimagnetic grain-size range as the discrete particles. The relative amounts of these two forms in any sample strongly influence the magnetic separation efficiencies because of the physics of the extraction process.

(5) Contrary to the findings of Sun & Jackson (1994), we find no evidence for significant dissolution of magnetite during acetic acid dissolution of the sample carbonate, even though we used more concentrated acid.

## ACKNOWLEDGMENTS

We are grateful to David Hallam who provided the extraction efficiencies for the early Pleistocene sediments from East Anglia, and Graham Shimmield who performed the XRF measurements for carbonate content. Andy Perkins provided lively comment. Pete Rowe designed and largely built the HGMS

equipment. This work was supported by a NERC(UK) research grant to BAM. Leg 117 and 115 samples were supplied with the assistance of the International Ocean Drilling Program. The XRD measurements were mostly performed in the Institute of Food Research, Norwich.

## REFERENCES

- Backman, J. *et al.*, 1988. *Proc. ODP Init. Repts.*, **115**, Ocean Drilling Program, College Station, TX.
- Bloemendal, J. & deMenocal, P., 1989. Evidence for a change in the periodicity of tropical climate cycles at 2.4 Myr from whole-core magnetic susceptibility measurements, *Nature*, **342**, 897–900.
- Bloemendal, J., King, J.W., Hunt, A., deMenocal, P.B. & Hayashida, A., 1993. Origin of the sedimentary magnetic record at Ocean Drilling Program sites on the Owen Ridge, Western Arabian Sea, *J. geophys. Res.*, **98**, 4199–4219.
- Canfield, D.E. & Berner, R.A., 1987. Dissolution and pyritisation of magnetite in anoxic marine sediments, *Geochim. cosmochim. Acta*, **51**, 645–659.
- Cummins, D.L., Himmelbau, D.A., Oberteuffer, J.A. & Powers, G.L., 1976. Capture of small paramagnetic particles by magnetic forces from low speed flows, *Am. Inst. Chem. Eng. J.*, **22**, 569–575.
- Evans, M.E. & Wayman, M.L., 1970. An investigation of small magnetic particles by electron microscopy, *Earth planet. Sci. Lett.*, **9**, 365–370.
- Freeman, R., 1986. Magnetic mineralogy of pelagic limestones, *Geophys. J. R. astr. Soc.*, **85**, 433–452.
- Geissman, J.M., Harlan, S.S. & Brearley, A.J., 1988. The physical isolation and identification of carriers of geologically stable remanent magnetisation: palaeomagnetic and rock magnetic microanalysis and electron microscopy, *Geophys. Res. Lett.*, **15**, 479–482.
- Hallam, D.F. & Maher, B.A., 1994. A record of reversed polarity carried by the iron sulphide, greigite in British early Pleistocene sediments, *Earth planet. Sci. Lett.*, **121**, 71–80.
- Heider, F., Korner, U. & Bitschere, P., 1993. Volcanic ash particles as carriers of remanent magnetisation in deep sea sediments from the Kerguelan Plateau, *Earth planet. Sci. Lett.*, **118**, 121–134.
- Hounslow, M., Maher, B.A. & Thistlewood, L., 1995. A magnetic mineral investigation of polarity reversals in a late Triassic sequence from the Beryl Basin, northern North Sea, in *Application of Paleomagnetism to the Oil Industry*, eds Turner, P. & Turner, A., Geological Society of London Special Publication, **98**, 119–147.
- Hughes, J.C., 1982. High-gradient magnetic separation of some soil clays from Nigeria, Brazil and Columbia. I. The inter-relationships of iron and aluminium extracted by acid ammonium oxalate and carbon, *J. Soil Sci.*, **33**, 509–519.
- Jackson, M.J., Rochette, P., Fillion, G., Banerjee, S.K. & Marvin, J., 1993. Rock magnetism of remagnetised palaeozoic carbonates: Low-temperature behaviour and susceptibility characteristics, *J. geophys. Res.*, **98**, 6217–6225.
- Karlin, R., 1990. Magnetic mineral diagenesis in sub-oxic sediments at Bettis Site W-N, NE Pacific Ocean, *J. geophys. Res.*, **95**, 4421–4436.
- Karlin, R. & Levi, S., 1985. Geochemical and sedimentological control of the magnetic properties of hemipelagic sediments, *J. geophys. Res.*, **90**, 10373–10392.
- Lovlie, R., Lowrie, W. & Jacobs, M., 1971. Magnetic properties and mineralogy of four deep sea cores, *Earth planet. Sci. Lett.*, **15**, 157–168.
- Lu, G., Marshak, S. & Kent, D.V., 1990. Characteristics of magnetic carriers responsible for Late Paleozoic remagnetisation in carbonate strata of the mid-continent, USA, *Earth planet. Sci. Lett.*, **99**, 351–361.
- McCabe, C. & Channell, J.E.T., 1994. Late Palaeozoic remagnetisation in limestones from the Craven basin (Northern England) and the

- rock magnetic fingerprint of remagnetised sedimentary carbonates, *J. geophys. Res.*, **99**, 4603–4612.
- McCabe, C., Van der Voo, R., Peacor, D.R., Scotese, C.R. & Freeman, R., 1983. Diagenetic magnetite carries ancient yet secondary remanence in some Paleozoic carbonates, *Geology*, **11**, 221–223.
- Maher, B.A., 1988. Magnetic properties of some synthetic sub-micron magnetites, *Geophys. J.*, **94**, 83–96.
- Maher, B.A. & Taylor, R.M., 1988. Formation of ultrafine-grained magnetite in soils, *Nature*, **336**, 368–370.
- Maher, B.A. & Thompson, R., 1992. Paleoclimatic significance of the mineral magnetic record of the Chinese loess and paleosols, *Quat. Res.*, **37**, 155–170.
- Maher, B.A., Thompson, R. & Zhou, L.P., 1994. Spatial and temporal reconstruction of changes in the Asian paleomonsoon—a new magnetic mineral approach, *Earth planet. Sci. Lett.*, **125**, 461–471.
- Morgan, G.E. & Smith, P.P.K., 1981. Transmission electron microscope and rock magnetic investigations of remanence carriers in a Precambrian metadolerite, *Earth planet. Sci. Lett.*, **53**, 226–240.
- Oldfield, F., 1994. Toward the discrimination of fine-grained ferrimagnets by magnetic measurements in lake and near-shore sediments, *J. geophys. Res.*, **99**, 9045–9050.
- Ozdemir, O. & Banerjee, S.K., 1982. A preliminary magnetic study of soil samples from west-central Minnesota, *Earth planet. Sci. Lett.*, **59**, 393–403.
- Petersen, N., von Dobeneck, T. & Vali, H., 1986. Fossil bacterial magnetite in deep sea sediments from the south Atlantic, *Nature*, **320**, 611–615.
- Prell, W.L., *et al.*, 1989. *Proc. ODP Init. Repts*, **117**, Ocean Drilling Program, College Station, TX.
- Righi, D. & Jadault, P., 1988. Improving soil clay mineral studies by high gradient magnetic separation, *Clay Mineral*, **23**, 225–232.
- Robinson, S.G., 1990. Applications of whole-core magnetic susceptibility measurements of deep-sea sediments: Leg 115 results, in *Proc. Ocean Drilling Program Sci. Results*, **115**, 737–771, eds Backman, J. *et al.*, Ocean Drilling Program, College Station, TX.
- Schulze, D.G. & Dixon, J.B., 1979. High gradient magnetic separation of iron oxides and other magnetic minerals from soil clays, *Soil. Sci. Soc. Am. J.*, **43**, 795–799.
- Suk, D., Van der Voo, R. & Peacor, D.R., 1993. Origin of magnetite responsible for remagnetisation of early Paleozoic limestones of New York state, *J. geophys. Res.*, **98**, 419–434.
- Sun, W. & Jackson, M.J., 1994. Scanning electron microscopy and rock magnetic studies of magnetic carriers in remagnetised early Paleozoic carbonates from Missouri, *J. geophys. Res.*, **99**, 2935–2942.
- Vali, H., von Dobeneck, T., Amarantidis, G., Forster, O., Morteani, G., Bachmann, L. & Petersen, N., 1989. Biogenic and lithogenic magnetic minerals in Atlantic and Pacific deep sea sediments and their palaeomagnetic significance, *Geol. Rundschau*, **78**, 753–764.
- Verosub, K.L., Fine, P., Singer, M.J. & Tenpas, J., 1994. Pedogenic and paleoclimatic interpretation of the magnetic susceptibility record of the Chinese Loess paleosols: Reply, *Geology*, **22**, 859–860.
- Von Dobeneck, T., 1985. *Gesteinsmagnetische Untersuchungen an tiefseesedimenten des Sudatlantiks*, Diplomarbeit Inst. Allg. Angew. Geophys., Ludw. Max. Univ., Munchen.
- Von Dobeneck, T., Peterson, N. & Vali, H., 1987. Bakterielle magneto-fossilien—Palaomagnetische und palaontologische spuren einer ungewöhnlichen bacteriengruppe, *Geowiss. in unserer Zeit*, **1**, 27–35.
- Walker, T.R., Larson, E.E. & Hoblitt, R.P., 1981. Nature and origin of haematite in the Moenkopi Formation (Triassic), Colorado plateau: a contribution to the origin of magnetisation in red beds, *J. geophys. Res.*, **86**, 317–334.
- Walker, M.M., Kirschvink, J.L., Perry, A. & Dizon, A.E., 1985. Detection, extraction and characterization of biogenic magnetite, in *Magnetite Biomineralisation and Magnetoreception in Organisms*, pp. 155–166, eds Kirschvink, J.L., Jones, D.S. & MacFadden, B.J., Plenum, New York.